Journal of Materials Chemistry A

Cite this: DOI: 10.1039/c0xx00000x

www.rsc.org/xxxxxx

PAPER

Single-material graded refractive index layer for improving the efficiency of III-V triple-junction solar cells

Chan Il Yeo[a], Hee Ju Choi[b], Young Min Song[c], Seok Jin Kang[d], and Yong Tak Lee[a,d]*

Received (in XXX, XXX) Xth XXXXXXXXX 20XX, Accepted Xth XXXXXXXXX 20XX

DOI: 10.1039/b000000x

We present a single-material titanium oxide (TiO_2) bi-layer antireflection coating (ARC) produced using an oblique angle deposition for improving the power conversion efficiency (PCE) of III-V compound semiconductor triple-junction (TJ) solar cells. Experimental demonstration of the porous TiO_2 layers and optical modelling by rigorous coupled-wave analysis indicate that bi-layer TiO_2 could be used as universal ARC for all known TJ stacks with various materials combination. The optimum TiO_2 bi-layer ARC produced on a $Ga_{0.5}In_{0.5}P/GaAs/Ge$ TJ solar cell exhibits the considerably enhanced PCE of 31.6%, which is higher than that of the cells without ARC (23.8%) and with TiO_2 single-layer ARC (29.1%). Incident angle-dependent device characteristics of the fabricated TJ solar cells are also discussed.

Introduction

III-V semiconductor based multi-junction (MJ) solar cells are promising candidates for achieving high power conversion efficiency (PCE) and for solar power plants and space applications due to their broadband absorption and strong durability.[1-5] A great deal of effort has been put into improving the PCE of III-V semiconductor MJ solar cells. To achieve high PCE, fundamentally, high photon absorption over the entire absorption spectrum of the solar cells is particularly essential. However, high Fresnel reflection losses originating from the large refractive index difference between air and the semiconductor material causes fewer photons to be transmitted into the solar cell.[4,6] In addition, photocurrent matching between series connected subcells, which is one of the most challenging issues in MJ solar cells, is crucial for improving their PCE.[1-4] This is because the net photocurrent of the MJ solar cell is determined by the subcell with the smallest photocurrent among the series connected subcells. To address this issue, finely designed surface antireflective structures have been investigated, which take into account the absorption spectrum of each subcell and the solar irradiance. This approach can effectively enhance the net photocurrent in the MJ solar cells and thereby improve the PCE. Commonly, multi-layer antireflection coatings (ARCs) with different optical materials have been widely used for surface antireflection. However, it has fatal drawbacks of very limited materials with suitable refractive indices and thermal mismatch.[7] Since there are no standard MJ stacks, materials selection issues are critical to the design and optimization of MJ solar cells.

Herein, we propose the use of versatile, single-material bi-layer ARCs with different refractive indices for improving the absorption efficiency of MJ solar cells. Porous titanium dioxide (TiO_2) bi-layer with different refractive indices were prepared by oblique angle deposition (OAD)[8-13] and directly employed on top of III-V semiconductor TJ solar cells with stacks of $Ga_{0.5}In_{0.5}P/GaAs/Ge$. The device performances (reflectance, cell efficiency, angle dependency, etc.) were systematically investigated. The experimental results and theoretical modeling of a TiO_2 bi-layer with different porosities showed that it is applicable to three 'representative' types of high-efficiency III-V semiconductor triple-junction (TJ) solar cells, i.e., $Ga_{0.5}In_{0.5}P/GaAs/Ge$, $Ga_{0.51}In_{0.49}P/Ga_{0.96}In_{0.04}As/Ga_{0.37}In_{0.63}As$, and $Ga_{0.35}In_{0.65}P/Ga_{0.83}In_{0.17}As/Ge$ TJ solar cells.[1]

Experimental and simulation modelling details

Fig. 1(a) shows a schematic illustration of a TJ solar cell with a TiO_2 bi-layer consisting of porous and dense TiO_2 films. The purpose of the bi-layer is to reduce unwanted surface reflection loss by introducing a graded refractive index ARC onto the outmost layer material (i.e., Aluminium Indium Phosphide, AlInP) of the solar cell. In this study, TiO_2 was deliberately employed as an optical material for ARC because it has a relatively high refractive index among various optical materials, which is a good feature for producing a graded refractive index ARC with a small difference in refractive index at the interface between the ARC and III-V semiconductor solar cells. In addition, TiO_2 is a highly transparent, nontoxic, and chemically and mechanically stable material.[14] TiO_2 ARC can be simply fabricated using general methods such as evaporation and sputtering of TiO_2 source as well as spin-coating of a colloidal solution containing TiO_2 nanoparticles.[14-15] Refractive index profiles of the TJ solar cells without and with the TiO_2 bi-layer ARC are shown in Fig. 1(b). It is clearly seen that the abrupt refractive index change from air (n_{air} = 1) to the outmost layer material of the TJ solar cell (n_{AlInP} ~2.98) is mitigated (two step graded) by employing the TiO_2 bi-layer ARC, resulting in the suppression of Fresnel reflection and thereby increasing photon absorption of the TJ solar cell. Fig. 1(c) shows the schematic of the OAD, which uses an electron-beam

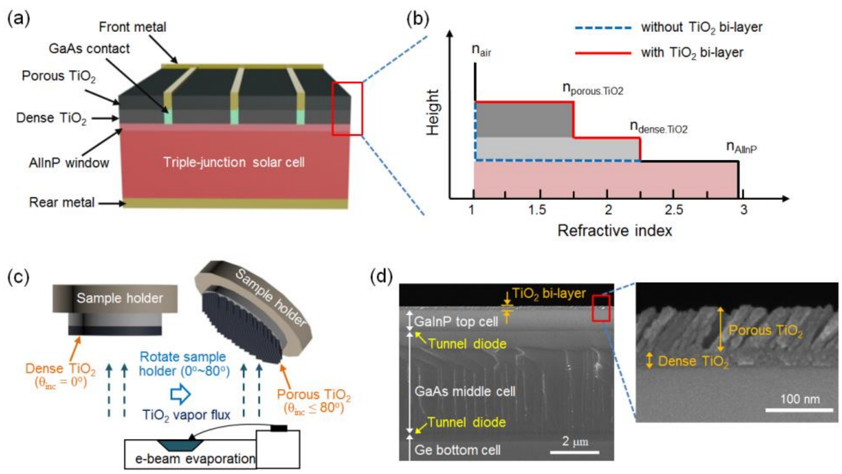

Fig. 1 (a) Schematic illustration of TJ solar cell with TiO_2 bi-layer. (b) Refractive index profiles of TJ solar cells without and with TiO_2 bi-layer. Refractive indices of each material at ~600 nm were considered. (c) Schematic of OAD of TiO_2 films. (d) SEM image of GaInP/GaAs/Ge TJ solar cell with TiO_2 bi-layer ARC.

(e-beam) evaporator. Dense TiO_2 film having a high refractive index was obtained by setting the incident vapor flux angle (θ_{inc}) as 0°. Porous TiO_2 films having lower low refractive indices were obtained by introducing air (porosity) within the deposited films by tilting the θ_{inc} up to 80° (i.e., with respect to substrate normal). Fig. 1(d) displays the cross-sectional view field-emission scanning electron microscope (FE-SEM, S-4700, Hitachi, Japan) images of a typical $Ga_{0.5}In_{0.5}P$/GaAs/Ge TJ solar cell with the TiO_2 bi-layer ARC produced using OAD. On the top surface of the solar cell, the dense and porous TiO_2 films deposited at an θ_{inc} of 0° and 80°, respectively, are clearly observed. The porous TiO_2 film with inclined nanocolumnar structures is the result of the nuclei formation and self-shadowing effect.[8,12] At the initial stage, evaporated adatoms condense onto the substrate and form nuclei, leaving shadowed regions and preventing the following vapor flux from entering the shadowed region. Consequently, nanocolumnar structures which are inclined in the direction of the incident vapor flux are produced.[8,12]

Prior to conducting theoretical calculations, the material properties of the oblique angle deposited TiO_2 films corresponding to θ_{inc} were investigated. Figs. 2(a)-2(b) reveal the cross-sectional view SEM images and the measured refractive indices (n) and extinction coefficients (k) of the TiO_2 films deposited at various θ_{inc}. It can be seen that the inclined angle of the deposited porous TiO_2 nanocolumnar structures become larger as the θ_{inc} increases, but smaller than θ_{inc}.[9,16] The measured refractive indices and extinction coefficients using spectroscopic ellipsometry (UVISEL, HORIVA, Japan) decrease due to the increased volume fraction of air within the deposited TiO_2 films with the increasing θ_{inc}. This result obviously indicates that the refractive index of an oblique angle deposited film can be engineered by adjusting the θ_{inc}. It is notable that the measured extinction coefficients of the deposited TiO_2 films are nearly zero for wavelengths above ~400 nm where most of the solar irradiance is distributed. This means that sunlight loss due to the TiO_2 ARC is not significant. From the refractive index measurement result, the porosity of the deposited TiO_2 film can be calculated using following equation:[11]

$$Porosity\ (\%) = \left(1 - \frac{n_{film}^2 - 1}{n_o^2 - 1}\right) \times 100 \quad (1)$$

where n_o (≈ 2.52) is the refractive index of pore-free anatase TiO_2,[16] and n_{film} is the measured refractive index of the deposited TiO_2 film. The calculated porosity of the TiO_2 films is presented in Table I. As expected, the calculated porosity of the TiO_2 films was increased from 24.1% to 61.5% as the θ_{inc} increased from 0° to 80° because of the increased volume fraction of air inside the TiO_2 films.

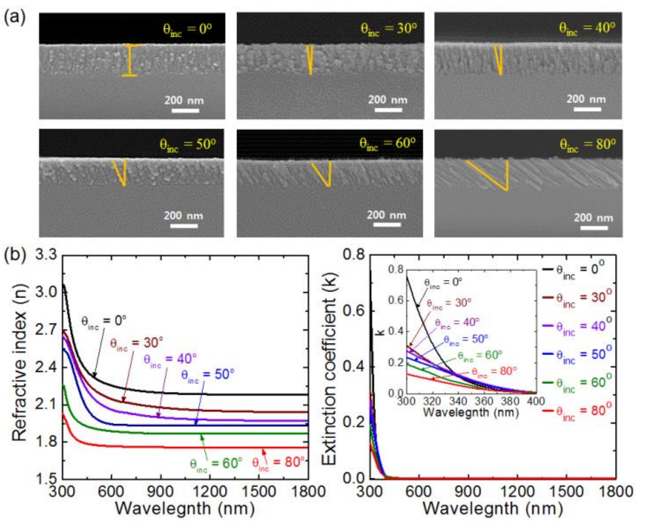

Fig. 2 (a) SEM images and (b) measured n and k of TiO_2 films deposited at various θ_{inc}. Inset is magnified graph in the wavelength range 300-400 nm.

Table I. Calculated porosity of deposited TiO_2 films for various θ_{inc}. Refractive indices of each material at ~600 nm were considered.

θ_{inc}	0	30	40	50	60	80
n	2.25	2.14	2.07	1.95	1.9	1.75
Porosity (%)	24.1	33.1	38.6	47.6	51.2	61.5

Fig. 3(a) displays schematic illustrations and the refractive index profiles of (i) $Ga_{0.5}In_{0.5}P$/GaAs/Ge (1.84/1.42/0.67 eV), (ii) $Ga_{0.51}In_{0.49}P$/$Ga_{0.96}In_{0.04}As$/$Ga_{0.37}In_{0.63}As$ (1.83/1.34/0.89 eV), and

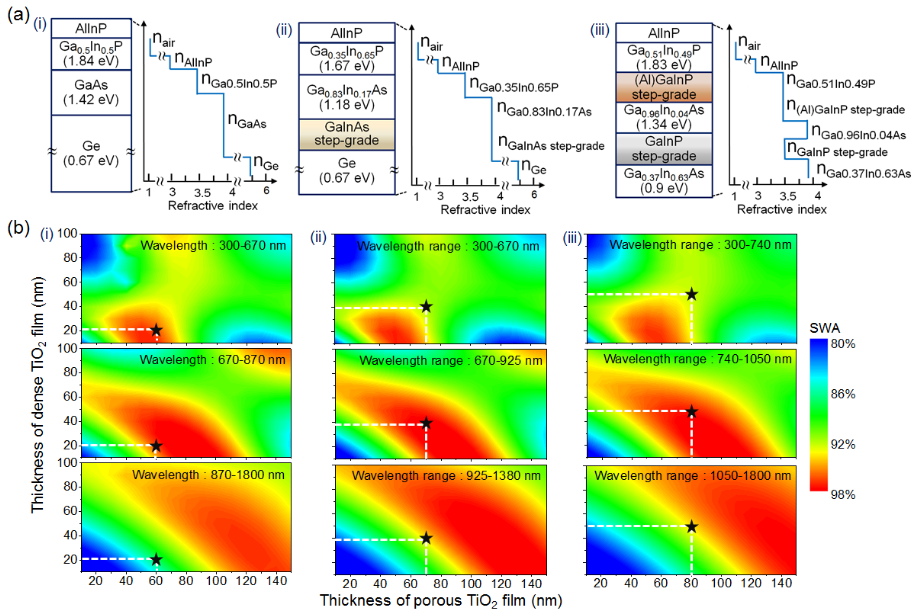

Fig. 3 (a) Schematic illustrations of cell designs and refractive index profiles of the three different TJ solar cells of (i) $Ga_{0.5}In_{0.5}P/GaAs/Ge$, (ii) $Ga_{0.51}In_{0.49}P/Ga_{0.96}In_{0.04}As/Ga_{0.37}In_{0.63}As$, and (iii) $Ga_{0.35}In_{0.65}P/Ga_{0.83}In_{0.17}As/Ge$. (b) Contour plots of the calculated SWAs of the TJ solar cells corresponding to the main absorption wavelength ranges of each subcell, and the thickness of dense ($n_{dense.TiO2}$ ~2.25) and porous ($n_{porous.TiO2}$ ~1.75) TiO_2 films.

(iii) $Ga_{0.35}In_{0.65}P/Ga_{0.83}In_{0.17}As/Ge$ (1.67/1.18/0.67 eV) TJ solar cells which can be found in the literature.[1,18-21] They have different combinations of materials, leading to different bandgap energy combinations (i.e., different light absorption ranges) and refractive index profiles. Fig. 3(b) shows contour plots of calculated solar-weighted absorption (SWA) corresponding to the main absorption wavelength ranges of each subcell and the thickness of the dense and porous TiO_2 films which were deposited at an θ_{inc} of 0° and 80°, respectively. Optical simulation based on the rigorous coupled-wave analysis (RCWA) method was performed to obtain the light absorption of the three different TJ solar cells with TiO_2 bi-layer ARCs to calculate the SWA.[22] Then, by considering the solar spectrum and the absorption spectrum of each subcell, the SWA was calculated using following equation:[4]

$$SWA = \frac{\int F(\lambda)A(\lambda)d\lambda}{\int F(\lambda)d\lambda} \quad (2)$$

where $F(\lambda)$ is the photon flux in the air mass 1.5 global (AM 1.5G) spectrum and $A(\lambda)$ is the calculated absorption.[23] For the RCWA simulation, the refractive indices of the compound semiconductor materials used were referenced,[24] and the step-grade layers were considered to be a transparent layer.[18,19] The net photocurrent in the $Ga_{0.5}In_{0.5}P/GaAs/Ge$ TJ solar cell is determined by the generated photocurrent in $Ga_{0.5}In_{0.5}P$ top cell or GaAs middle cell.[2,4] This is because the Ge bottom cell, which has much smaller bandgap energy compared to the other subcells, generates much higher photocurrent than other subcells. For this reason, i.e., current mismatching, the TiO_2 bi-layer ARC should be optimized to maximize the photon absorption both in the $Ga_{0.5}In_{0.5}P$ top cell and GaAs middle cell in order to enhance the net photocurrent, and thus improve the PCE of the TJ solar cell. Since the $Ga_{0.51}In_{0.49}P/Ga_{0.96}In_{0.04}As/Ga_{0.37}In_{0.63}As$ and $Ga_{0.35}In_{0.65}P/Ga_{0.83}In_{0.17}As/Ge$ TJ solar cells are current matched structures, therefore the TiO_2 bi-layer ARC should be designed to identically enhance photocurrents in three subcells simultaneously. From the SWA calculation results, TiO_2 bi-layer ARCs consisting of 20/60, 40/70, and 50/80 nm-thick dense and porous TiO_2 films having refractive indexes of $n_{dense.TiO2}$ ~2.25 and $n_{porous.TiO2}$ ~1.75 at ~600 nm were considered to be an optimum antireflective structure for effectively enhancing the net photocurrent (i.e., PCE) of the $Ga_{0.5}In_{0.5}P/GaAs/Ge$, $Ga_{0.51}In_{0.49}P/Ga_{0.96}In_{0.04}As/Ga_{0.37}In_{0.63}As$, and $Ga_{0.35}In_{0.65}P/Ga_{0.83}In_{0.17}As/Ge$ TJ solar cells TJ solar cells, respectively. We also carried out additional calculations using TiO_2 bi-layer ARCs consisting of more dense TiO_2 ($n_{dense.TiO2}$ ~2.4) and porous TiO_2 ($n_{porous.TiO2}$ ~1.5) films which can be found in literature.[11] The optimum thicknesses of TiO_2 bi-layer ARCs for the three representative types of TJ solar cells are presented in Table II.

Table II. Optimum thickness of TiO_2 bi-layer consisting of dense and porous TiO_2 films for various TJ solar cells.

TiO_2 bi-layer	$Ga_{0.5}In_{0.5}P/GaAs/Ge$	$Ga_{0.51}In_{0.49}P/Ga_{0.96}In_{0.04}As/Ga_{0.37}In_{0.63}As$[17,18]	$Ga_{0.35}In_{0.65}P/Ga_{0.83}In_{0.17}As/Ge$[19,20]
Dense (n ~2.25)/ Porous TiO_2 (n ~1.75)	20/60 nm	40/70 nm	50/80 nm
Dense (n ~2.4)/ Porous TiO_2 (n ~1.5)	40/80 nm	50/100 nm	50/80 nm

In this study, we verified the effect of the finely designed TiO_2 bi-layer ARC on the PCE improvement of the TJ solar cells by fabricating $Ga_{0.5}In_{0.5}P/GaAs/Ge$ TJ cells. The cells were monolithically grown on a p-type Ge substrate by metal-organic chemical vapor deposition system. TJ solar cells consisting of a 0.7 μm-thick $Ga_{0.5}In_{0.5}P$, 3.65 μm-thick GaAs, and 350 μm-thick Ge subcells and a 30 nm-thick AlInP window layer without ARC layer were prepared using following fabrication process. A Au/Ge/Ni/Au (20/50/10/300 nm) front metal electrode was deposited using an e-beam evaporator on a GaAs contact layer after removing native oxide using diluted HCl solution. The undesirable contact layer, except underneath the front electrode area, was selectively removed using the chemical etching method. Photolithography process was carried out to form a mesa pattern and then a multi-step chemical etching process was performed to etch the solar cell structure on to p-type Ge substrate. After forming a Ti/Pt/Au (20/20/300 nm) back metal electrode on the rear side of the TJ solar cell, the sample was annealed using a rapid thermal annealing system. After that, an optimum TiO_2 bi-layer ARC consisting of 20 nm-thick dense TiO_2 film followed by60 nm-thick porous TiO_2 film was deposited onto the surface of the TJ solar cell using OAD at an θ_{inc} of 0° and 80°, respectively. To prevent the deposition of TiO_2 onto metal busbars, the metal busbars were screened before depositing the TiO_2 films. For comparison, a TJ solar cell with an optimum 55 nm-thick dense TiO_2 single-layer ARC was also fabricated.

Results and discussion

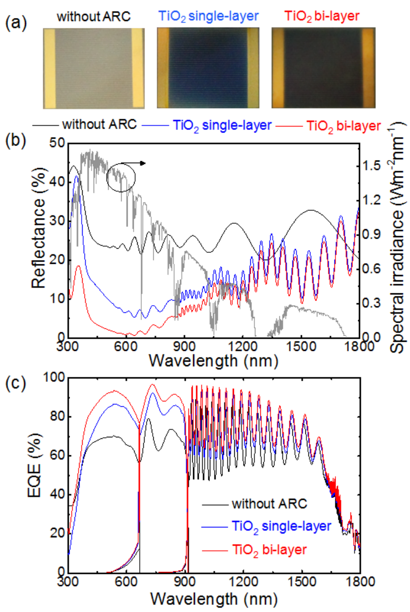

Fig. 4 (a) Photographs and (b) calculated reflection spectra and (c) EQE of the $Ga_{0.5}In_{0.5}P$/GaAs/Ge TJ solar cells without ARC, and with the optimum TiO_2 single- and bi-layer ARC.

Photographs of the fabricated TJ solar cells without and with optimum TiO_2 single- and bi-layer ARC are displayed in Fig. 4(a). The TJ solar cell with the TiO_2 bi-layer ARC appears nearly black because of its superior antireflection ability. In contrast, the cells without ARC and with a TiO_2 single-layer ARC show a gray and deep blue surface color due to their relatively poor antireflection property. Fig. 4(b) shows the reflectance spectra of the TJ solar cells. It can be obviously observed that the TJ solar cell with the optimum TiO_2 bi-layer has lower light reflection than the other solar cells over the entire wavelength range. The summarized solar-weighted reflectance (SWR)[6] of the three TJ solar cells corresponding to the main absorption spectrum of each subcell are shown in Table III. We also calculated the external quantum efficiency (EQE) of the TJ solar cells with and without TiO_2 ARC using a Silvaco ATLAS device simulator, as can be seen in Fig. 4(c). For an accurate EQE calculation, Shockly-Read-Hall recombination, Fermi-Dirac statistics, bandgap narrowing effect, and non-local tunnelling effect were considered. The TJ solar cell with the TiO_2 bi-layer ARC exhibited an increased EQE compared to the cells without ARC and with a TiO_2 single-layer ARC. In particular, the EQE improvement was prominent in the absorption wavelength ranges of the $Ga_{0.5}In_{0.5}P$ and GaAs subcells, which determine the net photocurrent of the TJ solar cell, due to the precisely designed TiO_2 bi-layer ARC for suppressing reflection loss in that wavelength range. Hence it is expected that the TJ solar cell with a TiO_2 bi-layer ARC may have an enhanced net photocurrent compared to other solar cells.

Table III. Calculated SWRs of the $Ga_{0.5}In_{0.5}P$/GaAs/Ge TJ solar cells without and with the optimum TiO_2 single- and bi-layer ARC corresponding to the main absorption wavelength range of each subcell.

Wavelength (nm)	without ARC (%)	TiO_2 single-layer (%)	TiO_2 bi-layer (%)
300-670	26.60	11.76	3.36
670-870	24.43	7.68	3.17
870-1800	26.11	15.44	12.73

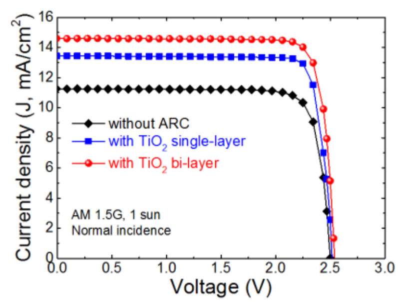

Fig. 5 Current density-voltage curves of $Ga_{0.5}In_{0.5}P$/GaAs/Ge TJ solar cells without and with optimum TiO_2 single- and bi-layer ARC.

We confirmed the photocurrent and PCE enhancement of the TJ solar cell with the TiO_2 bi-layer ARC by measuring current density-voltage (*J-V*) characteristics using a solar simulator (Sol3A, Oriel, USA) under one-sun of AM 1.5G illumination at room temperature. Fig. 5 shows the measured *J-V* curves of the fabricated TJ solar cells having an active area of 0.2858 cm^2. The TJ solar cell with the TiO_2 bi-layer ARC exhibited a short-circuit current (J_{sc}) of 14.60 mA/cm^2 which was a 29.7% and 8.7% enhanced J_{sc} compared to that without ARC (11.26 mA/cm^2) and with a TiO_2 single-layer ARC (13.43 mA/cm^2), respectively, because of the increased photon absorption as confirmed in Fig. 4(c). The open-circuit voltage (V_{oc}) of the TJ solar cells with ARCs was slightly increased, probably owing to the increased J_{sc}. This can be understood by the following equation,[13]

$$V_{oc} = \frac{E_g}{q} + \frac{NkT}{q}\ln(J_{sc}) - \frac{NkT}{q}\ln(J_0) \quad (3)$$

where E_g is the energy bandgap, N is the ideal factor, kT/q is the thermal voltage and J_0 is the saturation current density. It is observed that the fill factor (*FF*) of the TJ solar cells with TiO_2 ARC was also slightly increased. This presumably may be due to the surface passivation effect provided by the TiO_2 ARC. Overall, the TJ solar cell with TiO_2 bi-layer ARC exhibited an enhanced

PCE of 31.6% compared to that without ARC (23.8%) and with a TiO_2 single-layer ARC (29.1%), respectively. These results clearly show that the precisely designed TiO_2 bi-layer ARC with excellent antireflection properties can effectively enhance the net photocurrent and the PCE of TJ solar cells. The summarized characteristics of the TJ solar cells with and without TiO_2 ARC are presented in Table IV.

Table IV. Summarized characteristics of the $Ga_{0.5}In_{0.5}P$/GaAs/Ge TJ solar cells without and with optimum TiO_2 single- and bi-layer ARC.

Solar cell	V_{oc} (V)	J_{sc} (mA/cm^2)	*FF* (%)	PCE (%)
without ARC	2.512	11.26	84.2	23.8
TiO_2 single-layer	2.527	13.43	85.6	29.1
TiO_2 bi-layer	2.538	14.60	85.3	31.6

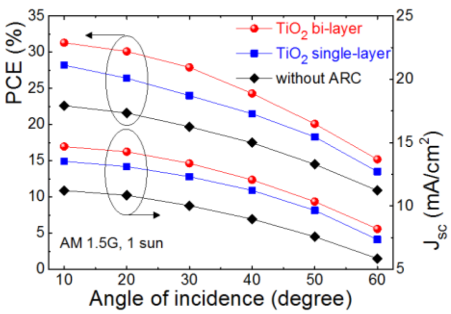

Fig. 6 Incident angle-dependent PCE and J_{sc} of the $Ga_{0.5}In_{0.5}P$/GaAs/Ge TJ solar cells without and with TiO_2 single- and bi-layer ARC.

The sun's altitude changes during the day. Thus, the incident angle-dependent PCE of a solar cell is important to ensure the stable generation of solar electricity during the daytime. The measured incident angle-dependent PCE and J_{sc} of the TJ solar cells without ARC and with optimum TiO_2 single- and bi-layer ARC are plotted in Fig. 6. It is noteworthy that the TJ solar cell with the TiO_2 bi-layer ARC exhibited the highest PCE for the entire angle of incidence (AOI, θ_i) among the three different cells. As the AOI was varied from 20° to 60°, the PCE of the solar cells without ARC and with TiO_2 single- and bi-layer decreased from 22.6% to 10.9%, 28.2% to 13.5%, and 31.3% to 15.2%, respectively. The efficiency drop is predominantly due to the decreased J_{sc} (11.22 to 5.86 mA/cm^2, 13.53 to 7.36 mA/cm^2, and 14.70 to 8.20 mA/cm^2 for the cells without and with TiO_2 single- and bi-layer ARC, respectively) with increasing AOI from 20° to 60°. Meanwhile, the decrease in J_{sc} can be attributed to the decline in incident sunlight into the solar cell proportional to $\cos\theta_i$ as well as increased surface reflection loss with an increase in the AOI. Although incident angle-dependent V_{oc} and *FF* were slightly decreased 0.157 ± 0.059 V and 3.93 ± 1.58%, respectively, as the AOI increased from 20° to 60°, these changes did not much affect the incident angle-dependent PCE of the TJ solar cells.

Conclusions

Single-material TiO_2 bi-layer ARCs produced by OAD were designed to maximize the PCE of three representative types of stacked TJ solar cells by taking into account the main absorption spectrum of each subcell and the solar irradiance. The $Ga_{0.5}In_{0.5}P$/GaAs/Ge TJ solar cell with an optimum TiO_2 bi-layer ARC having 20 nm-thick dense and 60 nm-thick porous TiO_2 films deposited at an θ_{inc} of 0° and 80°, respectively, exhibited considerably increased PCE of 31.6% compared to that of the cells without ARC (23.8%) and with a TiO_2 single-layer ARC (29.1%) under one-sun AM 1.5G illumination. This is predominantly due to the enhanced J_{sc} with the TiO_2 bi-layer ARC, compared to the cells without ARC and with a TiO_2 single-layer ARC. The finely designed TiO_2 bi-layer ARC has superior antireflection properties which enhances photon absorption in the current-limiting subcells (*i.e.*, $Ga_{0.5}In_{0.5}P$ and GaAs subcells). The TJ solar cell with the TiO_2 bi-layer ARC also exhibited a higher incident angle-dependent PCE than other solar cells in the AOI range from 20° to 60°. These results showed the great potential of versatile single-material graded refractive index ARC for effectively improving the PCE of various MJ solar cells without materials selection issues for ARC.

Acknowledgement

This work was supported by the National Research Foundation of Korea (NRF) grant funded by the Korea government (MEST) (No. 2011-0017606).

Notes and References

[a]*Advanced Photonics Research Institute, Gwangju Institute of Science and Technology, 1 Oryong-dong, Buk-gu, Gwangju, 500-712, Republic of Korea*
[b]*Department of Physics and Photon Science, Gwangju Institute of Science and Technology, 1 Oryong-dong, Buk-gu, Gwangju, 500-712, Republic of Korea*
[c]*Department of Electronics Engineering, Pusan National University, 2 Busandaehak-ro 63beong-gil, Geumjeong-gu, Busan, 609-735, Republic of Korea*
[d]*School of Information and Communications, Gwangju Institute of Science and Technology, 1 Oryong-dong, Buk-gu, Gwangju, 500-712, Republic of Korea*
Fax: +82-62-715-3128; Tel: +82-62-715-2278; E-mail: ytlee@gist.ac.kr

1 D. J. Friedman, *Curr. Opin. Solid State Mat. Sci.*, 2010, **14**, 131-138.
2 P. Yu, M. Y. Chiu, C. H. Chang, C. Y. Hong, Y. L. Tsai, H. V. Han, and Y. R. Wu, *Prog. Photovoltaics*, 2014, **22**, 300-307.
3 J. Tommila, V. Polojärvi, A. Aho, A. Tukiainen, J. Viheriälä, J. Salmi, A. Schramm, J. M. Kontio, A. Turtianiene, T. Niemi, and M. Guina, *Sol. Energy Mater. Sol. Cells*, 2010, **94**, 1845-1848.
4 C. I. Yeo, E. K. Kang, S. K. Lee, Y. M. Song, and Y. T. Lee, *IEEE Photonics J.*, 2014, **6**, 8400209.
5 C. N. Eisler, Z. R. Abrams, M. T. Sheldon, X. Zhang, and H. A. Atwater, *Energy Envrion. Sci.*, 2014, DOI: 10.1039/c4ee01060d.
6 C. I. Yeo, J. H. Kwon, S. J. Jang, and Y. T. Lee, *Opt. Express*, 2012, **20**, 19554-19562.
7 J. Q. Xi, M. F. Schubert, J. K. Kim, E. F. Schubert, M. Chen, S. Y. Lin, W. Liu, and J. A. Smart, *Nat. Photonics*, 2007, **1**, 176-178.
8 J. J. Steele and M. J. Brett, *J. Mater Sci.-Mater. Electron.* 2007, **18**, 367-379.
9 S. J. Jang, Y. M. Song, C. I. Yeo, C. Y. Park, J. S. Yu, and Y. T. Lee, *Opt. Express*, 2011, **19**, A108-A117.
10 J. W. Leem and Y. T. Lee, *Opt. Express*, 2011, **19**, A258-A268.
11 P. Mao, F. Sun, H. Yao, J. Chen, B. Zhao, B. Xie, M. Ham, and G. Wang, *Nanoscale*, 2014, **6**, 8177-8184.
12 P. Yu, C. H. Chang, C. H. Chiu, C. S. Yang, J. C. Yu, H. C. Kuo, S. H. Hsu, and Y. C. Chang, *Adv. Mater.*, 2009, **21**, 1618-1621.
13 L. K. Yeh, K. Y. Lai, G. J. Lin, P. H. Fu, H. C. Chang, C. A. Lin, and J. H. He, *Adv. Energy Mater.*, 2011, **1**, 506-510.
14 B. S. Richards, *Prog. Photovoltaics*, 2004, **12**, 253-281.

15 E. Shi, H. Li, L. Yang, L. Zhang, Z. Li, P. Li, Y. Shang, S. Wu, X. Li, J. Wei, K. Wang, H. Zhu, D. Wu, Y. Fang, and A. Cao, *Nano Lett.*, 2013, **13**, 1776-1781.
16. Y. Zhong, Y. C. Shin, C. M. Kim, B. G. Lee, E. H. Kim, Y. J. Park, K. M. A. Sobahan, C. K. Hwangbo, Y. P. Lee, and T. G. Kim, *J. Mater. Res.*, 2008, **23**, 2500-2505.
17 W. D. Kingery, H. K. Bowen, D. R. Uhlmann, *Introduction to Ceramics*, Wiley, New York, 1976, pp. 650-651.
18 J. F. Geisz, D. J. Friedman, J. S. Ward, A. Duda, W. J. Olavarria, T. E. Moriarty, J. T. Kiehl, M. J. Romero, A. G. Norman, and K. M. Jones, *Appl. Phys. Lett.*, 2008, **93**, 123505.
19 J. F. Geisz, A. X. Levander, A. G. Norman, K. M. Jones, and M. J. Romero, *J. Cryst. Growth*, 2008, **310**, 2339-2344.
20 W. Guter, J. Schöne, S. P. Philipps, M. Steiner, G. Siefer, A. Wekkeli, E. Welser, E. Oliva, A. W. Bett, and F. Dimroth, *Appl. Phys. Lett.*, 2009, **94**, 223504.
21 F. Dimroth, R. Beckert, M. Meusel, U. Schubert, and A. W. Bett, *Prog. Photovoltaics*, 2001, **9**, 165-178.
22 M. G. Moharam and T. K. Gaylord, *J. Opt. Soc. Am.*, 1981, **71**, 811-818.
23 NREL's AM1.5 Standard Dataset: http://rredc.nrel.gov/solar/spectra/am1.5/, Accessed 17 January 2014.
24 SOPRA, http://www.sopra-sa.com, Accessed 1 September 2013.

